

Ab initio calculation of *KL**V* Auger spectra in Si

Eric K. Chang and Eric L. Shirley

Optical Technology Division, National Institute of Standards and Technology, 100 Bureau Drive, Mail Stop 8441, Gaithersburg, Maryland 20899-8441

(Received 2 January 2002; revised manuscript received 28 February 2002; published 9 July 2002)

We present an *ab initio* Green's-function formalism for predicting *CCV* Auger spectra for solids. The formalism takes into account core-hole screening, final-state interaction effects, and angular momentum dependence. It is applied to calculate the *KL*₁*V* and *KL*_{2,3}*V* Auger spectra for bulk silicon. We achieve fair agreement with high-resolution Auger experiments recently performed on silicon and gain a more quantitative understanding of the role of the final-state hole-hole interaction in Auger processes.

DOI: 10.1103/PhysRevB.66.035106

PACS number(s): 79.90.+b

I. INTRODUCTION

In recent years, high-resolution measurements of *KL**V* Auger spectra for bulk silicon have been performed.¹ This experimental study revealed detailed features in the Auger spectra that had not been observed before in previous work.² Various theoretical analyses^{1,3,4} have been used to explain the observed spectra. These include computation of the partial density of states (PDOS) in the presence of a core hole and weighting the various angular momentum contributions by parameters fitted to experiment; and the use of the Cini-Sawatsky model,⁵ a Green's function approach with a model Hamiltonian and empirically determined parameters. These models have provided useful qualitative explanations of the observed spectra. A useful summary of these models is given in Ref. 6. These studies have left the field open to timely theoretical developments, including *ab initio* calculations of the angular-momentum-dependent matrix elements, screening of the core hole, and the Coulomb repulsion between the two final-state holes. *Ab initio* calculations, using configuration interaction⁷ and many-body perturbation theory (MBPT),⁸ have been performed on atoms, but to our knowledge *ab initio* calculations have yet to be performed for solids. In this work, we address these issues by developing an appropriate *ab initio* formalism for the calculation of the *KL*₁*V* and *KL*_{2,3}*V* Si Auger spectra. The calculation involves the following steps. First, the matrix elements for *KL**V* Auger decay in the Si atom are computed within the Hartree-Fock approximation using standard formulas. Next, we construct the matrix elements for *KL**V* Auger decay in the solid, where the final valence state is an extended Bloch state. The solid-state matrix elements are reconstructed from the atomic matrix elements. From a calculation of the band energies, wave functions, and the screened potential produced by the final-state core hole, we construct a two-particle Green's function that describes the dynamics of the two final-state holes, including their mutual repulsive interaction. The Auger intensity is directly related to this two-particle Green's function and the solid-state matrix elements. The characteristic features of our method consists of the *ab initio* calculation of final-state effects and the unified way in which the matrix-element and final-state effects are treated.

II. FORMALISM

We make use of Wentzel's rule⁹ for the transition rates of nonradiative processes. According to Wentzel, the probability amplitude of the Auger transition $(nl) \rightarrow (n_1l_1, n_2l_2) \epsilon_A l_A$, is given by the matrix element

$$\Pi_{i \rightarrow f} = \left\langle \Psi_f(nl, \epsilon_A l_A; \mathbf{r}_1 \mathbf{r}_2) \left| \frac{1}{|\mathbf{r}_1 - \mathbf{r}_2|} \right| \Psi_i(n_1 l_1, n_2 l_2; \mathbf{r}_1 \mathbf{r}_2) \right\rangle. \quad (1)$$

Here \overline{nl} , $\overline{n_1 l_1}$, $\overline{n_2 l_2}$, and $\epsilon_A l_A$ are the quantum numbers of the initial core hole, the two final-state holes, and the Auger electron. Because we are interested in developing a Green's function, many-body formalism, we rewrite Wentzel's rule in second-quantized notation. To this end, we consider matrix elements of the interaction Hamiltonian,

$$H_{int} = \frac{1}{2} \sum_{n_1 n_2 n_3 n_4 \sigma_1 \sigma_2} M_{n_3 n_4, n_1 n_2} \hat{c}_{n_4 \sigma_2}^\dagger \hat{c}_{n_3 \sigma_1}^\dagger \hat{c}_{n_1 \sigma_1} \hat{c}_{n_2 \sigma_2}. \quad (2)$$

Here n_1, n_2, n_3 , and n_4 are indices that label orbital states, and σ_1 and σ_2 are spin indices. Likewise, $\hat{c}_{n\sigma}^\dagger$ and $\hat{c}_{n\sigma}$ are fermion creation and annihilation operators satisfying the anticommutation relations

$$\{\hat{c}_{n_1 \sigma_1}^\dagger, \hat{c}_{n_2 \sigma_2}\} = \delta_{n_1 n_2} \delta_{\sigma_1 \sigma_2},$$

$$\{\hat{c}_{n_1 \sigma_1}, \hat{c}_{n_2 \sigma_2}\} = 0,$$

$$\{\hat{c}_{n_1 \sigma_1}^\dagger, \hat{c}_{n_2 \sigma_2}^\dagger\} = 0.$$

$M_{n_3 n_4, n_1 n_2}$ is given by the integral

$$M_{n_3 n_4, n_1 n_2} = \int d^3 r_1 d^3 r_2 \phi_{n_3}^*(\mathbf{r}_1) \phi_{n_4}^*(\mathbf{r}_2) \frac{1}{|\mathbf{r}_1 - \mathbf{r}_2|} \times \phi_{n_1}(\mathbf{r}_1) \phi_{n_2}(\mathbf{r}_2),$$

where the $\phi_n(\mathbf{r})$ are quasiparticle wave functions. We are interested in computing matrix elements of the Hamiltonian given in Eq. (2) between an initial state, $|i(\uparrow)\rangle$, and final states, $\{|f(\alpha\lambda\mu)\rangle\}$, given by

$$|i(\uparrow)\rangle = \hat{c}_{K\uparrow}|0\rangle,$$

$$|f(\alpha\lambda\mu)\rangle = \hat{c}_{A\alpha}^\dagger \hat{c}_{L\lambda} \hat{c}_{V\mu}|0\rangle.$$

Here A , L , and V label the orbitals for the Auger, L , and valence states, and α , λ , and μ are the respective spins. K refers to the K hole, which is assumed to be spin-up without loss of generality. The portion of the interaction Hamiltonian relevant to KL V Auger processes is

$$H_{KLV} = \sum_{n_1 n_2 \alpha} M_{AK, n_1 n_2} \hat{c}_{K\uparrow}^\dagger \hat{c}_{A\alpha}^\dagger \hat{c}_{n_1 \alpha} \hat{c}_{n_2 \uparrow}$$

with

$$M_{AK, n_1 n_2} = \int d^3 r_1 d^3 r_2 \phi_A^*(\mathbf{r}_1) \phi_K^*(\mathbf{r}_2) \frac{1}{|\mathbf{r}_1 - \mathbf{r}_2|} \times \phi_{n_1}(\mathbf{r}_1) \phi_{n_2}(\mathbf{r}_2).$$

The Auger amplitude is given by

$$\Pi(\alpha\lambda\mu) \equiv \langle f(\alpha\lambda\mu) | H_{KLV} | i(\uparrow) \rangle,$$

which reduces to

$$\begin{aligned} \Pi(\alpha\lambda\mu) &= \sum_{n_1 n_2} M_{AK, n_1 n_2} [\delta_{n_2 V} \delta_{n_1 L} \delta_{\mu\uparrow} \delta_{\lambda\alpha} \\ &\quad - \delta_{n_2 L} \delta_{n_1 V} \delta_{\mu\alpha} \delta_{\lambda\uparrow}] \\ &= M_{AK, LV} \delta_{\lambda\alpha} \delta_{\mu\uparrow} - M_{AK, VL} \delta_{\mu\alpha} \delta_{\lambda\uparrow}. \end{aligned}$$

Squaring this result and summing over final-state spins, we obtain

$$\begin{aligned} \sum_{\alpha\lambda\mu} |\Pi(\alpha\lambda\mu)|^2 &= |M_{AK, LV} - M_{AK, VL}|^2 + |M_{AK, LV}|^2 \\ &\quad + |M_{AK, VL}|^2. \end{aligned} \quad (3)$$

$M_{AK, LV}$ and $M_{AK, VL}$ are the direct and exchange matrix elements, later denoted by D and G in the atom and Δ and Γ in the solid. The result given in Eq. (3) is consistent with past works.^{10,11}

Having shown how to handle the exchange symmetry properly as in Eq. (3), we now develop the formalism for calculating the atomic matrix elements, i.e., the exchange and direct terms given by $M_{AK, VL}$ and $M_{AK, LV}$, where the four states involved, including the final valence-hole state, are atomic or atomiclike continuum states. It is necessary to compute the atomic matrix elements before writing down the matrix elements for the solid, in which the final valence-hole state is, without loss of generality, a linear combination of extended Bloch states. For purposes of computing Auger transition matrix elements, it is more convenient to describe the states in an atomic picture. For purposes of treating the final states, it is more convenient to describe the valence-hole state in a Bloch picture, *viz.* as a linear combination of Bloch states. To treat the entire problem in a unified fashion,

we relate the two pictures by expressing each Bloch state in the vicinity of an atom as a linear combination of atomic-like states.

The radial part of the atomic wave functions corresponding to the K hole, L hole, valence hole, and Auger electron, are designated by $K(r)$, $L(r)$, $V_{\nu l_2}(r)$, and $A_{l_a}(r)$. The total and azimuthal angular momentum quantum numbers for these states are designated as $l_c m_c$, $l_1 m_1$, $l_2 m_2$, and $l_a m_a$. The subscript c stands for ‘‘core hole,’’ and a stands for ‘‘Auger electron,’’ whereas ν is like the principal quantum number of the valence state. We define

$$K_{l_c, m_c}(\mathbf{r}) \equiv K(r) Y_{l_c, m_c}(\hat{\mathbf{r}})$$

$$L_{l_1, m_1}(\mathbf{r}) \equiv L(r) Y_{l_1, m_1}(\hat{\mathbf{r}})$$

$$V_{l_2, m_2}(\mathbf{r}) \equiv V_{\nu l_2}(r) Y_{l_2, m_2}(\hat{\mathbf{r}})$$

and

$$A_{l_a, m_a}(\mathbf{r}) \equiv A_{l_a}(r) Y_{l_a, m_a}(\hat{\mathbf{r}}).$$

The orbitals are computed within the Hartree-Fock approximation. Those for the Auger electron and K hole are calculated in the final-state configuration, and those for the two final-state holes, i.e., the valence and L holes, are computed in the initial-state configuration. This choice of configurations is consistent with the MBPT calculation of Ref. 8.

For fixed l_c , m_c , l_1 , and m_1 , the exchange and direct matrix elements are functions of ν , l_2 , and m_2 , the quantum numbers for the valence hole, and l_a and m_a , the quantum numbers for the Auger electron. They are given by

$$\begin{aligned} D_{\nu, l_2 m_2}^{l_a m_a} &= \int d^3 r d^3 r' K_{l_c m_c}^*(\mathbf{r}) L_{l_1 m_1}(\mathbf{r}) \frac{1}{|\mathbf{r} - \mathbf{r}'|} \\ &\quad \times V_{\nu l_2 m_2}(\mathbf{r}') A_{l_a m_a}^*(\mathbf{r}') \end{aligned} \quad (4)$$

and

$$\begin{aligned} G_{\nu, l_2 m_2}^{l_a m_a} &= \int d^3 r d^3 r' K_{l_c m_c}^*(\mathbf{r}) V_{\nu l_2 m_2}(\mathbf{r}) \frac{1}{|\mathbf{r} - \mathbf{r}'|} \\ &\quad \times L_{l_1 m_1}(\mathbf{r}') A_{l_a m_a}^*(\mathbf{r}'). \end{aligned} \quad (5)$$

Here $l_a m_a$ and $\nu l_2 m_2$ are taken to vary, and $l_1 m_1$ and $l_c m_c$ are constants depending on the spectrum studied (in the case of KL_1V Auger spectroscopy, they are $l_1=0, m_1=0$ and $l_c=0, m_c=0$). D and G are related by an exchange of the roles of the valence and L holes. They can be calculated explicitly using the following formulas:

$$\begin{aligned} D_{\nu, l_2 m_2}^{l_a m_a} &= \sum_{lm} \frac{4\pi}{2l+1} R_l[K, L, V_{\nu l_2}, A] g(l_c m_c; l_1 m_1 l m) \\ &\quad \times g^*(l_2 m_2; l_a m_a l m) \end{aligned} \quad (6)$$

and

$$G_{\nu,l_2m_2}^{l_a m_a} = \sum_{lm} \frac{4\pi}{2l+1} R_l[K, V_{\nu l_2}, L, A] g(l_c m_c; l_2 m_2 l m) \times g^*(l_1 m_1; l_a m_a l m) \quad (7)$$

with

$$R_l[a, b, c, d] \equiv \int_0^\infty dr \int_0^\infty dr' \frac{r^l}{r'^{l+1}} (rr')^2 \times a^*(r) b(r) c(r') d^*(r')$$

and

$$g(lm; l_1 m_1 l_2 m_2) = \int d\Omega Y_{lm}^*(\hat{\mathbf{r}}) Y_{l_1 m_1}(\hat{\mathbf{r}}) Y_{l_2 m_2}(\hat{\mathbf{r}}).$$

The solid-state (crystal) matrix elements, $\Delta_{n\mathbf{k}}^{l_a m_a}$ and $\Gamma_{n\mathbf{k}}^{l_a m_a}$, are like the atomic exchange matrix elements $D_{\nu, l_2 m_2}^{l_a m_a}$, and $G_{\nu, l_2 m_2}^{l_a m_a}$, except that the final valence hole is not an atomic state described by the quantum numbers ν , l_2 and m_2 , but a Bloch state with index $n\mathbf{k}$, where n and \mathbf{k} denote the band index and crystal momentum. We compute Bloch wave functions and their corresponding band energies within the local-density approximation (LDA),^{12,13} which is adequate for Si. Because Auger processes involve only valence bands (and no conduction bands), and the LDA gives satisfactory results for Si, self-energy corrections to the LDA band energies are small.¹⁴ The relationship between the solid-state matrix elements and the atomic matrix elements can be expressed as

$$\Delta_{n\mathbf{k}}^{l_a m_a} = \sum_{\nu l_2 m_2} c_{\nu l_2 m_2}^{n\mathbf{k}} D_{\nu, l_2 m_2}^{l_a m_a}, \quad (8)$$

and

$$\Gamma_{n\mathbf{k}}^{l_a m_a} = \sum_{\nu l_2 m_2} c_{\nu l_2 m_2}^{n\mathbf{k}} G_{\nu, l_2 m_2}^{l_a m_a}. \quad (9)$$

The transformation coefficients $\{c_{\nu lm}^{n\mathbf{k}}\}$ are given by

$$c_{\nu lm}^{n\mathbf{k}} = 4\pi \sum_{\mathbf{G}} i^l Y_{lm}(\hat{\mathbf{Q}}) c_{n\mathbf{k}}(\mathbf{G}) \tilde{V}_{\nu l}(Q)$$

with $\mathbf{Q} = \mathbf{G} + \mathbf{k}$,

$$\tilde{V}_{\nu l}(Q) = \int_0^\infty dr r^2 j_l(Qr) V_{\nu l}(r),$$

and $c_{n\mathbf{k}}(\mathbf{G})$ being a Fourier component of the Bloch state $n\mathbf{k}$. We compute the LDA wave functions and energies using pseudopotentials and a plane-wave basis set up to an energy cutoff of 16 Ry and with a k point sampling consisting of 10 k points in the irreducible Brillouin zone. Because we compute the wave functions using pseudopotentials, we make use of the wave function reconstruction method in Ref. 15, which relates pseudo and all-electron wave functions, and is used to reconstruct the latter. We estimate the standard un-

certainty in the peak heights of the final spectrum from the reconstruction process to be less than 5%.

To treat the interaction of the final-state holes, we follow the method of Ref. 16, in which inelastic x-ray scattering and absorption are studied. There, an attractive core hole-electron interaction was considered, while here a repulsive hole-hole interaction is considered. This method, when applied to Auger spectroscopy, retains the same qualitative features of the Cini-Sawatsky model⁵ and is its *ab initio* counterpart. It is also consistent with the final-state rule for Auger spectra,³ according to which the initial state determines the s -, p -, and d -wave Auger electron intensities, and the final state determines the individual shapes of each of these contributions. The key ingredient in this two-particle Green's-function method is the following effective Hamiltonian, which describes the dynamics of the two final-state holes (i.e., the L hole and the valence hole):

$$H_{n\mathbf{k}, n'\mathbf{k}'} = -\delta_{nn'} \delta_{\mathbf{k}\mathbf{k}'} (\epsilon_L^{OP} + \epsilon_{n\mathbf{k}}^{OP}) + K_{n\mathbf{k}, n'\mathbf{k}'}^d \pm K_{n\mathbf{k}, n'\mathbf{k}'}^x \quad (10)$$

with

$$K_{n\mathbf{k}, n'\mathbf{k}'}^d = \int d^3r W_L(r) \phi_{n'\mathbf{k}'}^*(\mathbf{r}) \phi_{n\mathbf{k}}(\mathbf{r})$$

and

$$K_{n\mathbf{k}, n'\mathbf{k}'}^x = \int d^3r' d^3r \phi_{n'\mathbf{k}'}^*(\mathbf{r}') L_{l_1, m_1}(\mathbf{r}') \frac{1}{|\mathbf{r}' - \mathbf{r}|} \times \phi_{n\mathbf{k}}(\mathbf{r}) L_{l_1, m_1}^*(\mathbf{r}).$$

The “+” sign in Eq. (10) is for spin singlet states and the “−” sign is for spin triplet states.²¹ W_L is the repulsive screened potential produced by the L core hole (2s or 2p). It is computed using the random-phase approximation with local-field effects, including self-consistent screening in the solid-state environment by core and valence electrons.^{16,22} The K^d term in Eq. (10) captures the effects of the direct interaction between the valence hole and L core hole. K^x is the exchange interaction between valence hole and L core hole, which has been found to be small and to change the spectra by only a few percent in the peak heights and less than 0.1 eV in the peak positions.

The final two-hole state can be represented in a band structure picture by a hole in the n th band at \mathbf{k} with energy $\epsilon_{n\mathbf{k}}^{OP}$, and an empty core level with energy ϵ_L . If the two holes did not interact, then the Hamiltonian would include only the first, energy-difference term in Eq. (10). However, because the two holes interact and may scatter into another two-hole pair state because of their mutual Coulomb repulsion, additional terms are required to describe the coupling between different two-hole pair states, i.e., between states labeled by $n\mathbf{k}, L$, and $n'\mathbf{k}', L$. The coupling is given by the sum or difference of the last two terms in Eq. (10).

Equation (10) is formally derived using an infinite ladder expansion of Feynman diagrams involving a pair of outgoing and a pair of incoming fermion lines, representing, in the case of this work, the two final-state holes. From this expan-

sion, an eigenvalue equation called the Bethe-Salpeter equation is derived, which is simply the eigenvalue problem associated with the Hamiltonian in Eq. (10). A complete and rigorous derivation of Eq. (10) is given in Ref. 23. An equation analogous to Eq. (10) has been applied to treat final-state interaction effects in inelastic x-ray spectra.¹⁶

The relevant two-particle Green's function is

$$G_{n\mathbf{k},n'\mathbf{k}'}(\omega) = (H - \omega + i\gamma)_{n\mathbf{k},n'\mathbf{k}'}^{-1},$$

where γ is related to the total inverse lifetime. We use

$$\gamma = \gamma_K + \gamma_L + \gamma_V,$$

with $\gamma_K = 0.38$ eV, $\gamma_{L_1} = 2.0$ eV, and $\gamma_{L_{2,3}} = 0.02$ eV, according to Refs. 17–19. For the inverse lifetime of the valence hole, γ_V , we use the results of self-energy calculations in Ref. 20.

Recalling Eq. (3), we can write down the final Auger intensity with the correct combination of direct and exchange matrix elements. If we define

$$\Sigma_{n\mathbf{k}}^{l_a m_a} = \Delta_{n\mathbf{k}}^{l_a m_a} - \Gamma_{n\mathbf{k}}^{l_a m_a},$$

then the Auger intensity $I(\omega)$ is

$$\begin{aligned} I(\omega) \propto & -\text{Im} \sum_{l_a m_a} \sum_{n\mathbf{k},n'\mathbf{k}'} \{ [\Sigma_{n\mathbf{k}}^{l_a m_a}]^* G_{n\mathbf{k},n'\mathbf{k}'}(\omega) \Sigma_{n'\mathbf{k}'}^{l_a m_a} \\ & + [\Delta_{n\mathbf{k}}^{l_a m_a}]^* G_{n\mathbf{k},n'\mathbf{k}'}(\omega) \Delta_{n'\mathbf{k}'}^{l_a m_a} \\ & + [\Gamma_{n\mathbf{k}}^{l_a m_a}]^* G_{n\mathbf{k},n'\mathbf{k}'}(\omega) \Gamma_{n'\mathbf{k}'}^{l_a m_a} \}. \end{aligned}$$

In the numerical calculation of $I(\omega)$, we sum over a k-point mesh consisting of 512 k points in the full Brillouin zone.

III. RESULTS

To understand the final results better, we first resolve the total Auger intensity into contributions from s , p , and d Auger electrons for both the KL_1V and $KL_{2,3}V$ spectra. An elementary calculation of the angular momentum coupling reveals that, in the case of the KL_1V Auger process, an s Auger electron leaves behind an s valence hole, a p Auger electron leaves behind a p valence hole, while higher values of angular momentum are less important. For the $KL_{2,3}V$ Auger process, s and d Auger electrons can leave behind a p valence hole, and p Auger electrons can leave behind an s valence hole, while higher values of angular momentum are less important.

In Fig. 1, we show the KL_1V Auger spectrum resolved into its Auger s and p contributions. They resemble the s and p PDOS (Ref. 1) for Si in the presence of a core hole, as expected. The sum of these two components, shown in Fig. 2, has a three-peak structure. The middle peak is the extremum of the sum of the two components and does not appear as a local maximum in either component.

In Fig. 3, we show the $KL_{2,3}V$ Auger spectrum resolved into its Auger s , p , and d contributions. The valence p portion of the spectrum is significantly more intense than the valence s portion, and most of the intensity is associated with a

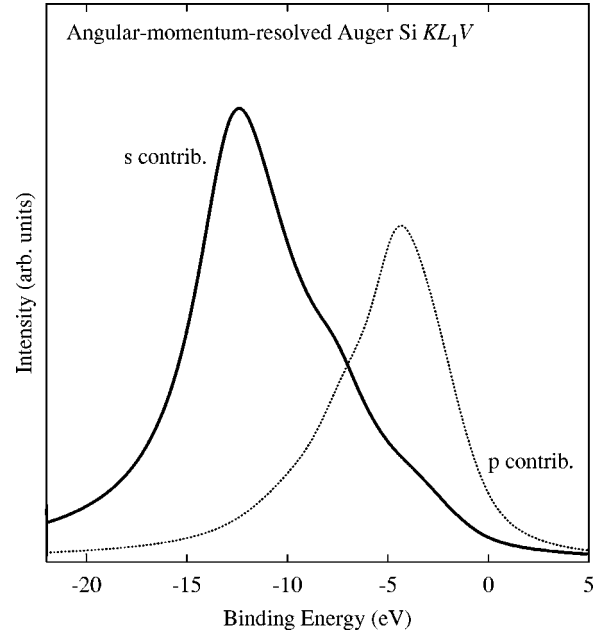


FIG. 1. KL_1V Auger intensity resolved into s (solid line) and p (dotted line) Auger electron contributions.

d -wave Auger electron. The sum of the two contributions is given in Fig. 4. The Auger s and d contributions resemble the p PDOS and the Auger p contribution resembles the s PDOS, as expected.

It is interesting to superpose the Auger spectrum computed with the final-state hole-hole interaction over the spectrum computed without such an interaction. In the KL_1V spectrum (Fig. 2), the hole-hole interaction has the effect of deepening the valley between the two main peaks and causes

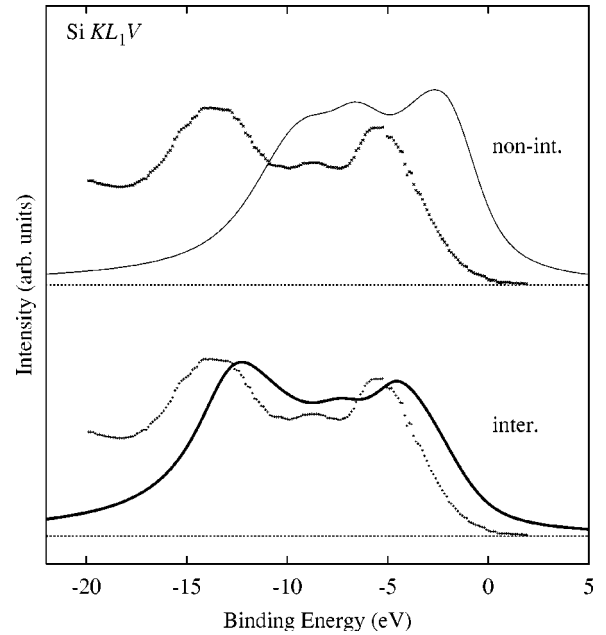


FIG. 2. Comparison of KL_1V theory with (bold line) and without (light line) hole-hole interaction to experiment [1] (points). The theoretical spectra are vertically offset for clarity.

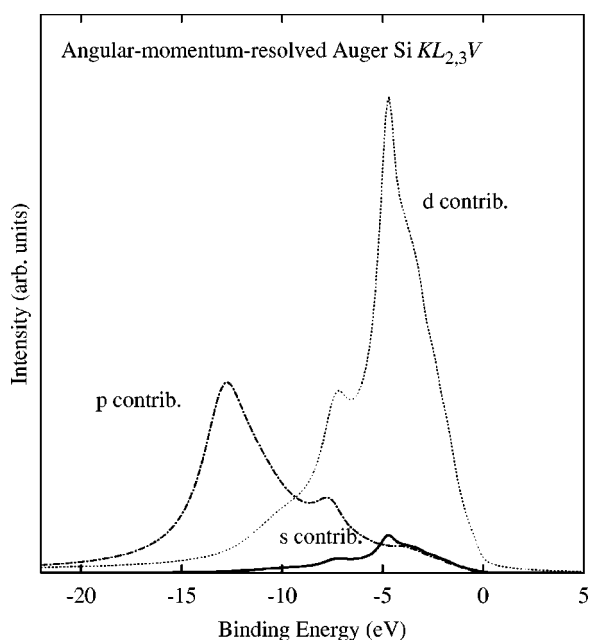


FIG. 3. $KL_{2,3}V$ Auger intensity resolved into s (solid line) and p (dotted-dashed line) and d (dotted line) Auger electron contributions.

a marked improvement in the agreement with experiment. In the $KL_{2,3}V$ spectrum (Fig. 4), the hole-hole interaction gives rise to the characteristic small peak to the left of the main peak. This feature is absent in the noninteracting theory. Finally, for both the KL_1V and $KL_{2,3}V$ spectra, the final-state hole-hole interaction shifts the peaks towards the same energies of the experimentally observed peaks. To our knowledge, this is the first fully *ab initio* calculation of the Auger Si KL_V intensity that includes energy-dependent, solid-state matrix elements and the final-state interaction together in a unified picture.

IV. CONCLUSION

We have presented a first-principles method for calculating the CCV Auger profile, which takes into account matrix-element and final-state effects. We have applied this method to the calculation of KL_1V and $KL_{2,3}V$ Auger spectra for bulk Si and achieved fair agreement with experiment. We reproduce approximately the peak shapes, relative heights,

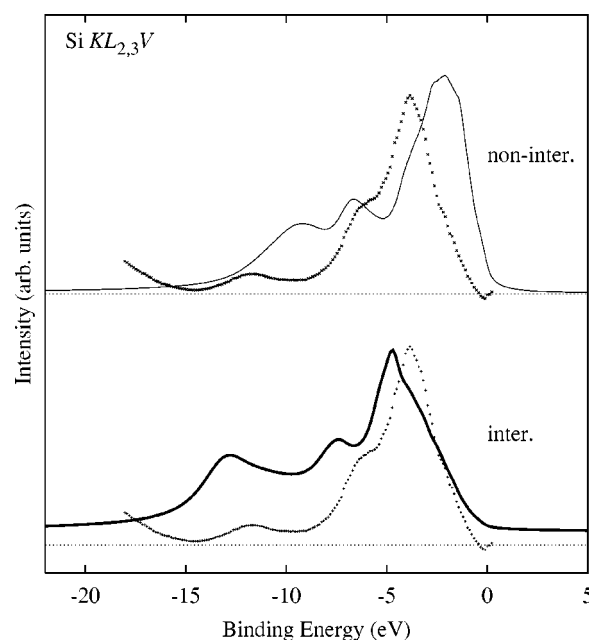


FIG. 4. Comparison of $KL_{2,3}V$ theory with (bold line) and without (light line) hole-hole interaction to experiment [1] (points). The theoretical spectra are vertically offset for clarity.

and positions as well as the fine features observed experimentally. In agreement with previous, more empirical work, we confirm that final-state effects are crucial in the calculation of Auger spectra, and our spectra were obtained with no adjustable parameters. We have also found that $KL_{2,3}V$ Auger decay in Si appears to produce predominantly d Auger electrons. It remains to note that we have neglected the coupling between electrons and plasmons. Such coupling gives rise to processes in which Auger electrons lose energy through the creation of plasmons. A complete qualitative discussion of this effect is found in section (3) of Ref. 6, where it has been shown that the electron-plasmon coupling modifies the Auger spectrum by the addition of a plasmon background. That is, the spectrum has an additional component that accounts for Auger electrons that have lost energy, introducing spectral weight at seemingly higher binding energies. An *ab initio* calculation of these plasmon effects would be an important development in future work. We note, however, that the present treatment still accounts for most of the observed spectral features.

¹P.S. Fowles, J.A. Evans, P.M. Lee, A.D. Laine, and P. Weightman, Phys. Rev. B **48**, 14 142 (1993).

²R. Lasser and J.C. Fuggle, Phys. Rev. B **22**, 2637 (1980).

³D.E. Ramaker, F.L. Hutson, N.H. Turner, and W.N. Mei, Phys. Rev. B **33**, 2574 (1986).

⁴T. Yamamoto and M. Uda, J. Electron Spectrosc. Relat. Phenom. **87**, 187 (1998).

⁵M. Cini, Phys. Rev. B **17**, 2486 (1978).

⁶M. Cini, C. Verdozzi, and A. Marini, J. Electron Spectrosc. Relat. Phenom. **117-118**, 41 (2001).

⁷W.N. Asaad, Nucl. Phys. **66**, 494 (1965).

⁸H.P. Kelly, Phys. Rev. A **11**, 556 (1975).

⁹G. Wentzel, Z. Phys. **43**, 524 (1927).

¹⁰P.J. Feibelman, E.J. McGuire, and K.C. Pandey, Phys. Rev. B **15**, 2202 (1971).

¹¹D.R. Jennison, Phys. Rev. B **18**, 6865 (1978).

¹²P. Hohenberg and W. Kohn, Phys. Rev. **136**, 864 (1964).

¹³W. Kohn and L.J. Sham, Phys. Rev. **140**, 1133 (1965).

¹⁴M.S. Hybertsen and S.G. Louie, Phys. Rev. B **34**, 5390 (1986).

¹⁵P.E. Blöchl, Phys. Rev. B **50**, 17 953 (1994); E.L. Shirley,

- S.I. Merritt, and J.A. Soininen (unpublished).
- ¹⁶J.A. Soininen and E.L. Shirley, Phys. Rev. B **64**, 165112 (2001), and references therein.
- ¹⁷E.J. McGuire, Phys. Rev. A **2**, 273 (1970).
- ¹⁸E.J. McGuire, Phys. Rev. A **3**, 587 (1971).
- ¹⁹E.J. McGuire, in *Atomic Inner Shell Processes*, edited by B. Crasemann (Academic, London, 1975), Vol. 1.
- ²⁰A. Fleszar and W. Hanke, Phys. Rev. B **56**, 10 228 (1997).
- ²¹J.C. Phillips, Phys. Rev. **123**, 420 (1961).
- ²²M.S. Hybertsen and S.G. Louie, Phys. Rev. B **35**, 5585 (1987).
- ²³A.L. Fetter and J.D. Walecka, *Quantum Theory of Many-Particle Systems* (McGraw-Hill, New York, 1971), Chap. 15, Eqs. (60.20)–(60.35).